ISSN 2543-9901

JOURNAL OF CASTING & MATERIALS ENGINEERING

AGH UNIVERSITY OF SCIENCE AND TECHNOLOGY
FACULTY OF FOUNDRY ENGINEERING

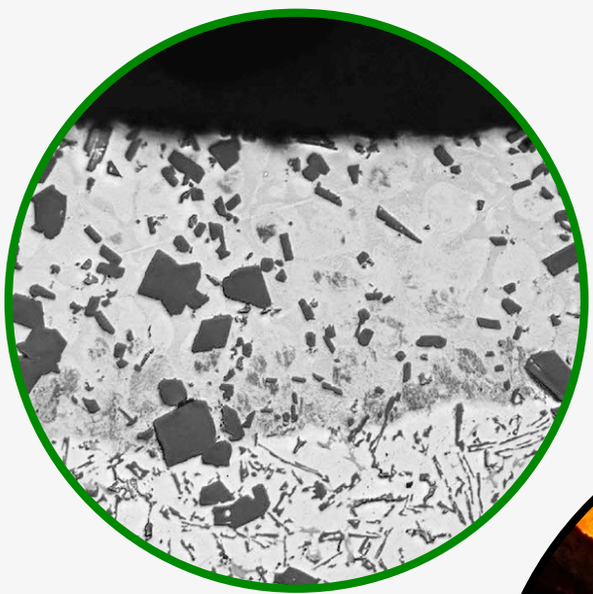

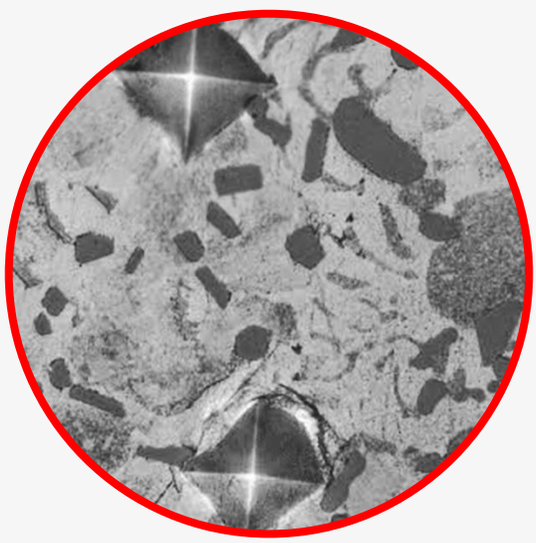

QUARTERLY
Vol.3 No.4/2019

JCME

AGH UNIVERSITY OF SCIENCE AND TECHNOLOGY PRESS KRAKOW 2019

The articles published in the Journal of Casting & Materials Engineering have been given a favorable opinion by the rewievers designated by the Editorial Board.

www:
https://journals.agh.edu.pl/jcme/

AGH UNIVERSITY OF SCIENCE AND TECHNOLOGY PRESS KRAKOW 2019

Wydawnictwa AGH (AGH University of Science and Technology Press)
al. A. Mickiewicza 30, 30-059 Kraków
tel. 12 617 32 28, 12 638 40 38
e-mail: redakcja@wydawnictwoagh.pl
http://www.wydawnictwa.agh.edu.pl

Contents

Journal of Casting & Materials Engineering Vol. 3 No. 4 (2019) 67–70
https://doi.org/10.7494/jcme.2019.3.4.67

Fabrication of Surface Layer Enriched with Zinc on AlSi17 Aluminium Cast Alloy by Hot-Dip Galvanizing

Tomasz Bucki[a]*, Dana Bolibruchová[b]

[a]Kielce University of Technology, Faculty of Mechatronics and Mechanical Engineering, Tysiąclecia Państwa Polskiego 7 Ave., 25 314 Kielce, Poland
[b]University of Zilina, Department of Technological Engineering, Univerzitna 8215/1 St., 010 26 Zilina, Slovakia
e-mail: tbucki@tu.kielce.pl

Received: 5 September 2019/Accepted: 21 January 2020/ Published online: 31 January 2020
This article is published with open access at AGH University of Science and Technology Press

Abstract

The paper deals with the fabrication of the surface layer enriched with Zn on AlSi17 aluminium alloy to modify the microstructure and surface properties of the alloy. The continuous surface layer was fabricated on the AlSi17 substrate by the hot-dip galvanizing of AlSi17 for 15min in a Zn bath heated to 450°C. The thickness of the layer was about 100 μm. The layer was characterised by a multi-component microstructure containing the regions of a solid solution of Al in Zn and dendrites of a eutectoid composed of a solid solution of Al in Zn and a solid solution of Zn in Al. In the layer, fine particles of Si with a regular shape were distributed. The results indicated that these Si particles formed by the action of Zn on the eutectic Si precipitations in the AlSi17 substrate. In the microstructure, large primary Si crystals and multi-phase precipitations, originating from the substrate, were also observed. The surface layer had much higher microhardness than the AlSi17 substrate. The results showed that hot-dip galvanizing can be used to modify the microstructure and properties of the surface layer of AlSi17. The study indicates the possibility of conducting further research on the fabrication of joints between AlSi17 and other metallic materials using a Zn interlayer fabricated by hot-dip galvanizing.

Keywords:

aluminium alloy, zinc, surface layer, hot-dip galvanizing, microstructure, microhardness

1. INTRODUCTION

Aluminium cast alloys are used in many fields of the industry due to their low density, combined with favourable casting and mechanical properties. The vast majority of aluminium alloys are characterised by good corrosion resistance in the natural atmosphere, sea water and many other chemical compounds [1, 2]. The good corrosion resistance is a result of the presence of a thin layer of aluminium oxide on the surface. This layer is a tight barrier preventing the aggressive action of the atmosphere on the metal. However, joining the aluminium alloys with other metals is difficult because of the occurrence of a passive layer on the surface. The layers enriched with zinc on the surface of the aluminium alloys are fabricated to improve the properties of the joints between them and other metallic materials. The literature data include the studies on the effect of a Zn interlayer on the microstructure and properties of pure Al or Al alloy combined with other metals such as Mg [3–8] or Cu [9], fabricated by brazing [3], friction stir welding [4], diffusion bonding [5], welding [6, 7], compound casting [8] or ultrasonic welding [9]. The combination of an Al alloy with other metals with the use of a Zn interlayer requires the enrichment of the Al surface with Zn prior to the joining process. The layers enriched with Zn on Al alloys can be produced by hot-dipping [3–5], diffusion bonding [8] electrolysis [10–12], or electroless deposition [10, 13]. Some methods allow the application of Zn between Al alloy and other metal during joining process [6, 7, 9].

According to Al-Si phase diagram [14], the AlSi17 alloy is a hyper-eutectic alloy. The microstructure of such an alloy contains the eutectic composed of Si (the solubility of Al in Si is negligibly low) and a solid solution of Si in Al. In the eutectic, primary Si crystals are distributed. The content of impurities, alloying elements and solidification conditions may cause the occurrence of additional structural components. Analysis of Al-Si [14], Al-Zn [15], Si-Zn [16] and Al-Si-Zn [17] phase diagrams shows that the addition of Zn to

the AlSi17 alloy can lead to significant changes in the structure. In the Al-Zn system at 381°C the eutectic transformation occurs. The product of this transformation is a eutectic composed of a solid solution of Al in Zn and a β′ phase, which is stable at high temperatures. Further cooling leads to the eutectoid transformation at 277°C, where β′ phase transforms to a eutectoid mixture composed of a solid solution of Al in Zn and a solid solution of Zn in Al [15, 17]. The authors of Si-Zn [16] and Al-Si-Zn [17] diagrams identified that the solubility of Zn in Si and Si in Zn is negligibly low.

The presented work includes the analysis of the microstructure and phase composition of the surface layer enriched with zinc on an AlSi17 aluminium cast alloy by hot-dip galvanizing and the determination of the effect of Zn on the microhardness of the layer.

2. EXPERIMENTAL PROCEDURE

AlSi17 aluminium cast alloy (17.18% Si, 1.22% Mg, 0.82% Ni, 0.72% Cu, 0.25% Fe, 0.02% Zn, balance of Al) was selected as the substrate material. Specimens with dimensions of 20 × 10 × 10 mm were cut out from the ingot. The surfaces of the specimens were prepared by means of grinding with abrasive papers up to 800 grit and cleaning in ethanol. The bath for hot-dipping was prepared by melting Zn (99.995% Zn) in a graphite crucible. The process parameters were selected on the basis of the tests and literature data. The surface layer enriched with zinc on AlSi17 was fabricated by dipping of the specimens for 15 min in a Zn bath heated to 450°C. After taking them out of the bath, the specimens were cooled in the air.

The cross-sections for microscopic observations were prepared by cutting the specimens using a low speed precision cutting machine and grinding them with an automatic grinding and polishing machine. Final polishing was performed using 0.3 μm polycrystalline alumina polishing suspension. Microscopic observations were conducted for non-etched specimens and after etching in 5% solution of sulfuric acid in a Nikon ECLIPSE MA 200 Optical Microscope (OM). The chemical composition was analysed in a JEOL JSM-7100F Scanning Electron Microscope connected with an energy dispersive X-ray spectroscopy (SEM/EDS). The phase composition of the surface layer enriched with Zn on AlSi17 was analysed by EDS analysis on the basis of Al-Si, Al-Zn, Si-Zn and Al-Si-Zn phase equilibrium diagrams [14–17]. The microhardness was measured by means of the Vickers method at a load of 50 g, using an Innovatest Nexus 4000 microhardness tester.

3. RESULTS AND DISCUSSION

Figure 1a shows the microstructure of the surface layer enriched with zinc on AlSi17 fabricated by hot-dip galvanizing at 450°C for 15 min, observed in OM without etching. The microstructure indicates that as a result of the contact of AlSi17 with molten Zn, the continuous surface layer with a thickness of about 100μm was formed on the AlSi17 substrate. The etching of the specimen revealed the complex structure of the layer (Fig. 1b).

Figure 2 presents the results of EDS linear analysis executed throughout the surface layer and the distribution of Al, Si and Zn. From the results, it is clear that as it moves from the AlSi17 substrate to the outer part of the layer, the Zn content increases, while the amount of Al decreases. In the produced layer, the content of Si is observed around the dark areas.

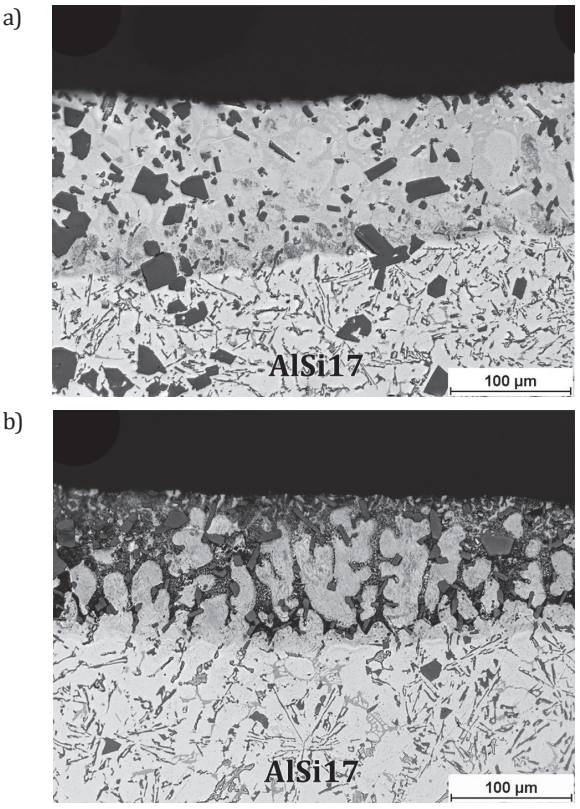

Fig. 1. OM images of the surface layer enriched with zinc on AlSi17 fabricated by hot-dip galvanizing: a) non-etched specimen; b) specimen after etching

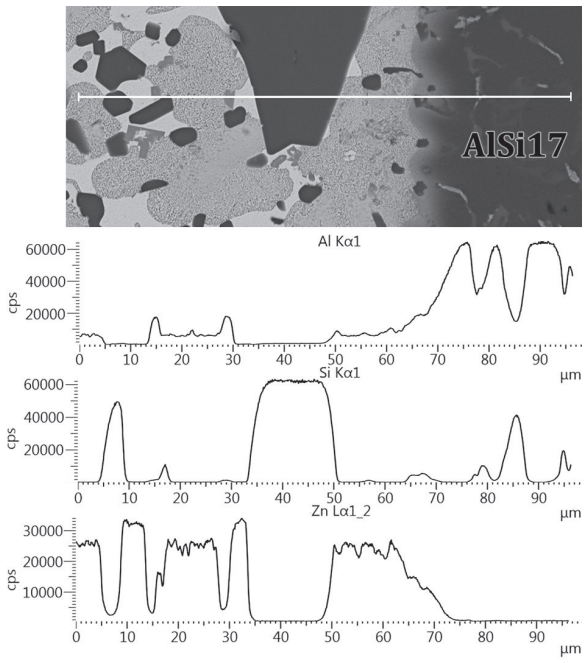

Fig. 2. Results of EDS linear analysis throughout the surface layer presenting the distribution of Al, Si and Zn

Figure 3 shows the SEM image of the inner part of surface layer with marked points where the chemical composition was examined by means of EDS analysis. The results of the analysis are summarised in Table 1.

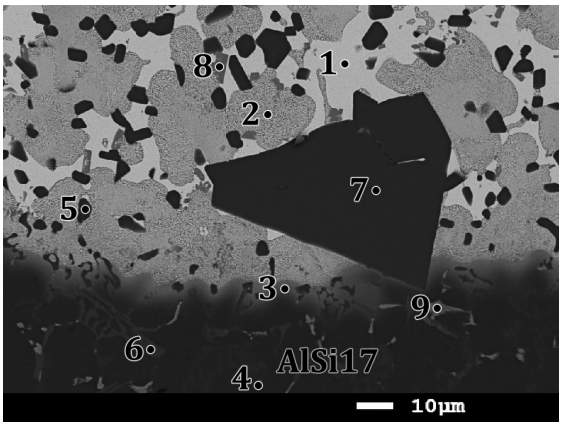

Fig. 3. SEM image of the inner part of the surface layer with the points where the chemical composition was analysed (explanation 1–9 in text)

The microstructure of the analysed part of the layer consisted mainly of the white areas with two-phase dendrites and dark particles. The composition in point 1 indicated that the white areas are composed of a solid solution of Al in Zn. The results for the dendrite marked as 2 corresponded to the composition of a eutectoid composed of a solid solution of Al in Zn and a solid solution of Zn and probably Si in Al. The analysis of the chemical composition of the substrate in the immediate vicinity of the layer (point 3) and at the depth of about 30 µm from the layer (point 4) showed that the AlSi17 substrate contained a solid solution of Si in Al and it was enriched with Zn in the region immediately adjacent to the layer. Subsequent results suggested that dark particles marked as 5 are Si precipitations. The comparison of the shape of these particles with the form of precipitations of eutectic Si in the AlSi17 substrate (marked as 6) indicated that during the fabrication of the layer, the Zn affects the precipitations of eutectic Si and, consequently, leads to their shape changing to a more regular one. The composition of the large, dark particle marked as 7 shows that it is composed of Si. The observation in SEM revealed that this Si particle is a primary Si crystal from the substrate, and the Zn during fabrication of the layer did not affect it visibly. The layer also contained fine, grey particles, marked as 8. The results of the analysis showed that their composition is similar to the composition of the multi-component phase containing Mn and Fe located in the substrate, marked as point 9.

In the outer part of the layer, shown in Figure 4, a slightly different microstructure was observed. The results of the EDS analysis from the regions marked in the figure are listed in Table 1. Close to the surface, the two-phase grey precipitations with an elongated shape (point 10) coexisted with the white areas, marked with the number 11. The results for the grey areas indicated a eutectoid (a solid solution of Al in Zn and a solid solution of Zn and probably Si in Al, while the chemical composition of the white areas corresponded to a solid solution of Al in Zn. The results of the analysis of the microstructure and phase diagrams [15, 17] suggest that the elongated shape of the eutectoid precipitations on the background of a solid solution of Al in Zn may be a result of the eutectic transformation that occurs during solidification.

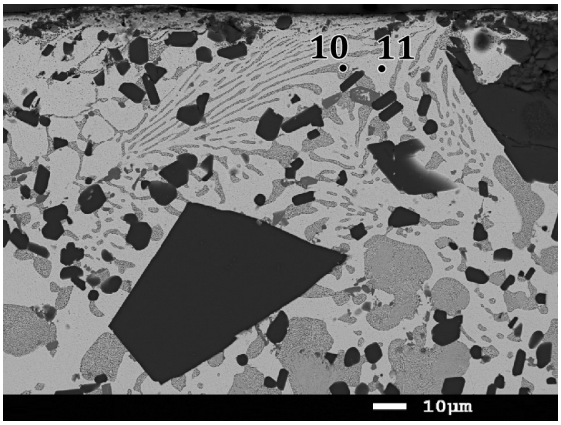

Fig. 4. SEM image of the outer part of the surface layer with the points where the chemical composition was analysed (explanation 10 and 11 in text)

Table 1
Results of EDS quantitative point analysis [at.%]

Point	Al	Si	Zn	Other
1	3.03	–	96.97	–
2	39.04	0.34	60.62	–
3	87.63	1.10	11.27	–
4	98.37	1.63	–	–
5	0.51	99.49	–	–
6	0.37	99.61	0.02	–
7	0.17	99.83	–	–
8	67.71	13.93	3.14	Mn: 5.48, Fe: 9.74
9	70.64	13.29	–	Mn: 6.11, Fe: 9.96
10	44.87	0.23	54.90	–
11	3.56	–	96.44	–

Figure 5 shows the traces of the Vickers microhardness measurements in representative regions of the produced layer and the AlSi17 substrate. The result obtained for the substrate was 65.3HV0.05, while in the surface layer enriched with Zn, the microhardness was much higher and rose to 96.1–104.4 HV0.05.

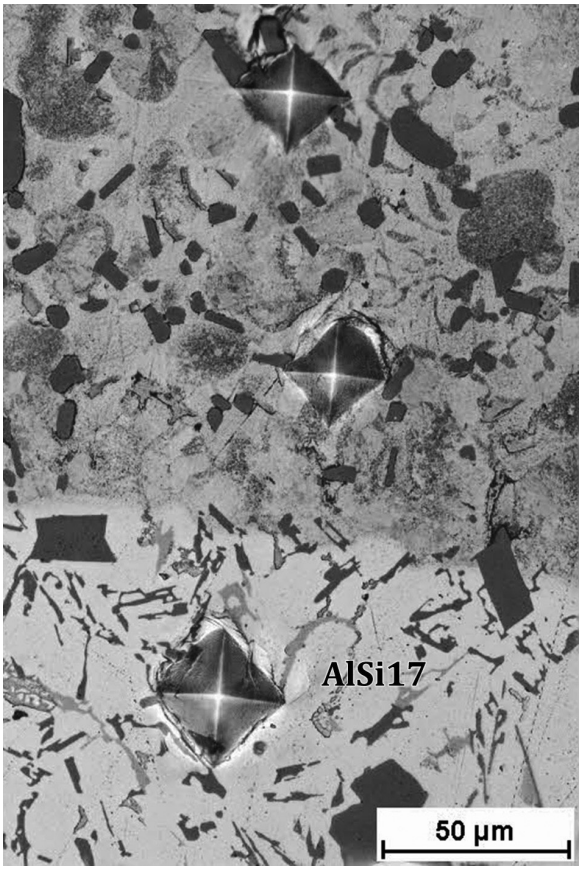

Fig. 5. Surface layer enriched with Zn on AlSi17 with traces of the Vickers microhardness measurements

The results of the study showed that continuous surface layer enriched with Zn was fabricated on the AlSi17 substrate by the hot-dip galvanizing process. The layer was characterised by a uniform thickness and higher microhardness than the AlSi17 substrate. The properties of the surface layer indicate its potential for further research focused on the fabrication of joints between AlSi17 and other metallic materials using an Zn interlayer fabricated by hot-dip galvanizing.

4. CONCLUSIONS

The surface layer enriched with Zn, characterised by a uniform thickness of about 100 µm, was formed on the AlSi17 substrate as a result of the specimens being dipped for 15 min in a Zn bath heated to 450°C. The analysis of the microstructure indicated that the layer had a multi-component microstructure containing the regions of a solid solution of Al in Zn and dendrites composed of a eutectoid (a solid solution of Al in Zn and a solid solution of Zn in Al). The layer contained fine particles of an Si, regular in shape, formed, according to the results, by the action of Zn on the precipitations of eutectic Si in the AlSi17 substrate. In the layer, large primary Si crystals and multi-phase precipitations originating from the substrate were also observed. In the microstructure, a thin region of the substrate immediately adjacent to the layer where the solid solution of Si in Al was enriched with Zn was observed. The surface layer was characterised by much higher microhardness in comparison with the AlSi17 substrate.

REFERENCES

[1] Hatch J.E. (1984). *ALUMINUM. Properties and Physical Metallurgy*. Ohio: American Society for Metals.
[2] Pastircak R., Scury J., Bruna M. & Bolibruchová D. (2017). Effect of Technological Parameters on the AlSi12 Alloy Microstructure during Crystallization under Pressure. A*rchives of Foundry Engineering,* 17(2), 75–78. Doi: 10.1515/afe-2017-0054
[3] Liu L., Tan J. & Liu X. (2007). Reactive brazing of Al alloy to Mg alloy using zinc-based brazing alloy. *Materials Letters*, 61, 2373-2377. Doi:10.1016/j.matlet.2006.09.016
[4] Xu R.Z., Ni D.R., Yang Q., Liu C.Z. & Ma Z.Y. (2016). Influence of Zn coating on friction stir spot welded magnesium-aluminium joint. *Science and Technology of Welding and Joining*, 22(6), 512–519. Doi: 10.1080/13621718.2016.1266735
[5] Zhao L.M. & Zhang Z.D. (2008). Effect of Zn alloy interlayer on interface microstructure and strength of diffusion-bonded Mg–Al joints. *Scripta Materialia*, 58(4), 283–286. Doi: 10.1016/j.scriptamat.2007.10.006
[6] Zhang H.T. & Song J.Q. (2011). Microstructural evolution of aluminum/magnesium lap joints welded using MIG process with zinc foil as an interlayer. *Materials Letters*, 65, 3292–3294. Doi: 10.1016/j.matlet.2011.05.080
[7] Zhang H.T., Dai X.Y. & Feng J.C. (2014). Joining of aluminum and magnesium via pre-roll-assisted A-TIG welding with Zn interlayer. *Materials Letters*, 122, 49–51. Doi: 10.1016/j.matlet.2014.02.008
[8] Mola R., Bucki T. & Gwozdzik M. (2018). The Effect of a Zinc Interlayer on the Microstructure and Mechanical Properties of a Magnesium Alloy (AZ31)–Aluminum Alloy (6060) Joint produced by Liquid–Solid Compound Casting. J*ournal of Minerals, Metals & Materials Society,* 71(6), 2078–2086. Doi: 10.1007/s11837-019-03405-y
[9] Balasundaram R., Patel V.K., Bhole S.D. & Chen D.L. (2014). Effect of zinc interlayer on ultrasonic spot welded aluminum-to-copper joints. *Materials Science and Engineering: A*, 607(3), 277–286. Doi: 10.1016/j.msea.2014.03.135
[10] Keller F. & Zelley W.G. (1950). Conditioning Aluminum Alloys for Electroplating. *Journal of the Electrochemical Society*, 97(4), 143–151. Doi: 10.1149/1.2777981
[11] Zelley W.G. (1953). Formation of Immersion Zinc Coatings on Aluminum. *Journal of the Electrochemical Society*, 100(7), 328–333. Doi: 10.1149/1.2781127
[12] Saidman S.B., Munoz A.G. & Bessone J.B. (1999). Electrodeposition of indium and zinc on aluminium. *Journal of Applied Electrochemistry*, 2, 245–251. Doi: 10.1039/c8gc03389g
[13] Wu J., Chen Z., Si Y.S., Guo Z.C. & Sun X.I. (2011). Two-Step Electroless Zinc Plating Process of 1060 Aluminum. *Materials Protection*, 607(05), 37–39.
[14] Murray J.L. & McAlister A.J. (1984). The AI-Si (Aluminum-Silicon) System. *Bulletin of Alloy Phase Diagrams*, 5, 74–84. Doi: 10.1007/BF02868729
[15] Murray J.L. (1983). The Al-Zn (Aluminum-Zinc) System. *Bulletin of Alloy Phase Diagrams*, 4, 55–73. Doi: 10.1007/BF02880321
[16] Olesinski R.W. & Abbaschian G.J. (1985). The Si-Zn (Silicon-Zinc) system. *Bulletin of Alloy Phase Diagrams*, 6, 545–548. Doi: 10.1007/BF02887156
[17] Jacobs M.H.G. & Spencer P.J. (1996). A critical thermodynamic evaluation of the systems Si-Zn and Al-Si-Zn. *Calphad*, 20(3), 307–320. Doi: 10.1016/S0364-5916(96)00033-8

Journal of Casting & Materials Engineering Vol. 3 No. 4 (2019) 71–75
https://doi.org/10.7494/jcme.2019.3.4.71

Characteristics of Wastes Produced by Polish Ferrous Alloys Casting Foundries between the Years 2010–2014

Mateusz Skrzyński*

AGH University of Science and Technology, Faculty of Foundry Engineering, Reymonta St. 23, 30-059 Krakow, Poland
e-mail: mskrzyns@agh.edu.pl

Received: 12 December 2019/Accepted: 15 January 2020/ Published online: 31 January 2020
This article is published with open access at AGH University of Science and Technology Press

Abstract

The balance of wastes originating from the foundry processes of ferrous alloys, prepared on the basis of data made available by the Polish Central Statistical Office, is presented in this paper. The kind and amount of individual foundry wastes subjected to management and storage by foundry plants were analysed. The problem of wastes between the years 2010–2016 is discussed on the national scale, as well as in individual regions or voivodeships. Altogether, 27,375.9 tons of waste from the group no. 10, of which non-ferrous metal and ferrous alloy wastes from foundry plants constituted 2%, were produced in Poland in 2010. This situation remained at a similar level over successive years, till 2014. The positive prognosis constitutes the fact that the amount of waste stored on dumping grounds belonging to foundry plants in Poland is gradually decreasing. This may be related to increasing costs of waste storage. During the tested years, the annual amount of gathered waste decreased from 4,796.6 thousand tons (in 2010) to 4,477.6 thousand tons (in 2014).

Keywords:

spent foundry sands, casting wastes, environment protection

1. INTRODUCTION

Founding is an efficient technique of manufacturing metal products with a specific shape and properties. It is based on filling the casting mold of the product with an alloy. Unfortunately, it belongs to the group of technologies which carry with them an increased occupational risk. Employees are exposed to harmful factors caused, among others, by the emission of harmful substances [1–4] during the process. The highest level of harmful substance emissions occurs during the pouring of disposable forms with iron alloys with a high melting temperature [5, 6]. In this case, one uses sand molds with sand grains connected by a binder. When filling the mold with liquid metal, a part of the binder burns out. Depending on the type of resin used, compounds from the BTEX group may be formed, such as benzene, toluene ethylbenzene, o-, m-, p-xylene), formaldehyde furfuryl alcohol phenol or polycyclic aromatic hydrocarbons (PAH) [7–9].

For the production of non-ferrous castings of zinc, aluminum, magnesium and copper alloys for the process, high pressure machines are more often used and the filled permanent mold is used to make a large number of castings. In this case, the amount of dangerous compounds generated during the foundry process is significantly reduced, together with the amount of waste generated [10].

The second important factor related to the topic of the article, and at the same time a challenge in terms of environmental protection for all foundry technologies, is the amount of waste generated during the production of castings.

Waste materials considered in the paper include:

- spent foundry and core sands,
- slag from the melting processes of liquid metals,
- dusts from cleaning out the furnaces for metal melting,
- other wastes generated during process the casting production process.

In Poland, as of 2014, there has been a change in the approach to the classification of waste generated and the separation of the method of managing this waste as transferred to other recipients. Therefore, the data concerning wastes produced and neutralised or subjected to the reclamation process in 2014, is not comparable with the data from previous years. From this year onwards, waste which is managed by its producers are counted as reclaimed and harmless wastes.

2. ANALYSIS OF THE AMOUNTS OF WASTE

Amounts of produced wastes and their management constitutes an important aspect in casting production. As sources estimate [2], for 1 ton of casting, approximately 1 ton of waste – requiring recycling or storage in special dumping grounds – is produced.

The main wastes at casting productions are wastes from moulds and cores [11–19], which on average constitute 77% of all wastes [20, 21]. A diagram presenting the percentages of various wastes from foundry processes is shown in Figure 1.

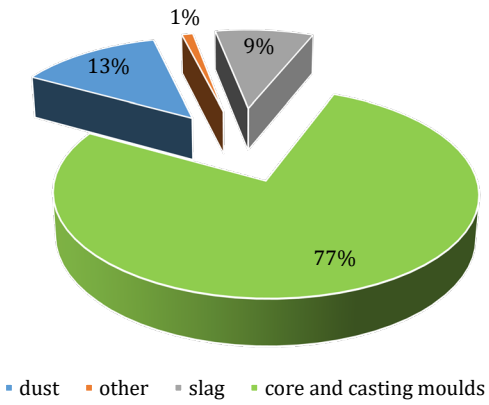

Fig. 1. Amount of waste from foundry processes in 2016 (in percent) [21]

Altogether 27 375.9 thousand tons of wastes from the group no. 10 were produced in Poland in 2010. 2% of these wastes constituted wastes from non-ferrous metals and ferrous alloys castings. This situation remained at a similar level up to the year 2016. Figure 2 presents the amount of waste produced by non-ferrous metal and ferrous alloys castings between the years 2010–2016.

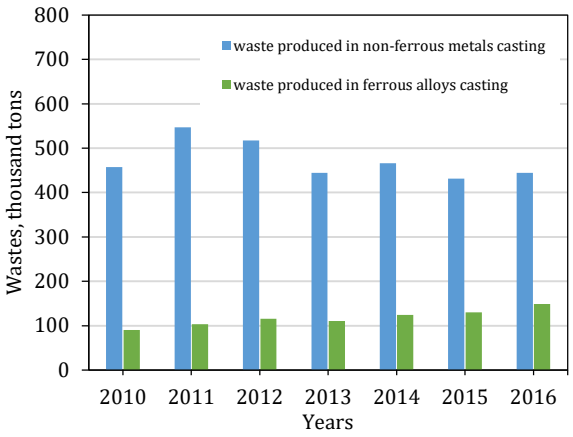

Fig. 2. Waste production by non-ferrous metal and ferrous alloys castings between the years 2010–2016 [21]

According to the report of the Polish Central Statistical Office, the production of waste from ferrous alloys casting in the analyzed years amounted to an average of 595.768 thousand tons and constituted the main source of waste. The amounts of waste originating from non-ferrous metal castings increased slightly during this period.

The largest amounts of waste in Poland were produced in the Silesian, Lesser Poland, Greater Poland and Warmian-Masurian voivodeships. The list of the amount of waste by individual voivodeships is presented in Table 1.

Table 1
List of waste produced by ferrous alloys casting in individual voivodeships in 2016 [22–28]

Voivodeship	Year						
	2010	2011	2012	2013	2014	2015	2016
Silesian	107.2	137.8	156.9	123.7	129.8	80.0	140.3
Lesser Poland	82.7	94.2	68.1	63.1	57.8	57.7	57.6
Greater Poland	77.9	97.5	96.7	67.6	70.6	55.7	53.0
Warmian-Masurian	68.4	65.2	63	55.7	76	63.5	67.8
Lower Silesian	24.6	28.6	28.1	35.4	36.7	67.5	21.0
Subcarpathian	20.5	25.1	21.7	19.8	20.1	26.0	23.5
Lodz	17.6	31.1	30.5	25.8	21.5	23.7	21.3
Holy Cross	15.8	14.7	14.1	23	25	23.5	24.7
Masovian	10.9	11.2	–	–	–	–	–
Opole	8.8	21.1	12.4	5.7	6.3	7.7	9.7
Lubusz	7.6	7.1	7.3	9.1	9.7	10.3	10.2
Lublin	7.2	4.2	10.7	8.2	5	8.0	9.1
Kuyavian-Pomeranian	5.1	7	6	5.8	5.8	5.4	4.7
Pomeranian	2.1	1.8	1.5	2.6	1.6	1.5	1.3
Podlaskie	0.9	0.7	0.6	–	–	26.0	–
West Pomerania	–	–	–	–	–	–	–

The largest amount of waste was produced in the years 2011 and 2012 [22, 23]. These data, combined with the casting production, are shown in Figure 3.

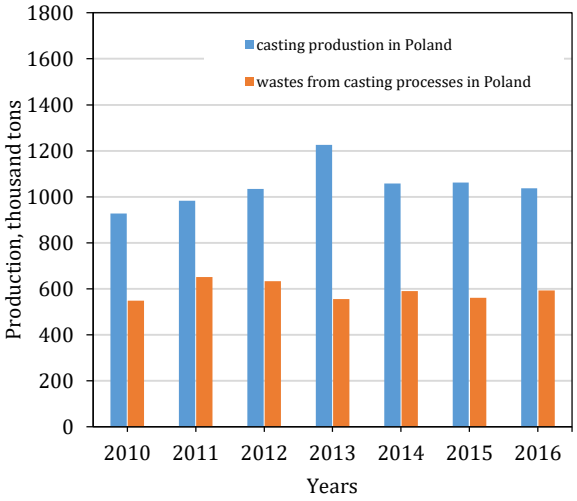

Fig. 3. The compilation of the casting production and the amount of waste related to this production between the years 2010–2016 [22–28]

The highest amounts of foundry wastes were reclaimed in 2016 in the Warmian-Masurian voivodeship and amounted to 50.8 thousand tons, or more than 75% of the total for the voivodeship. By comparison, Lesser Poland subjected 62% to reclamation, Silesia only 25% and Greater Poland only 1%. The total data are given in Figure 4. Foundry plants in the latter voivodeship had the largest amounts of wastes stored in their own dumping grounds, which in 2010 amounted to 1846.2 thousand tons. Very similar amounts were collected by foundry plants in the Opole voivodeship (1848.1 thousand tons). Between the years 2010–2016, the situation in these two voivodeships was at the similar level and in 2016 it was 1673.5 and 1243.6 thousand tons, respectively. The situation for 2016 is presented in Figure 5.

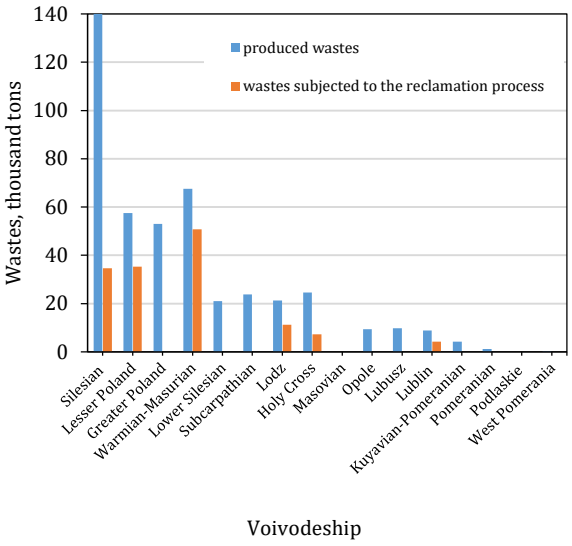

Fig. 4. The distribution of wastes produced and subjected to reclamation in individual voivodeships in 2016 [21]

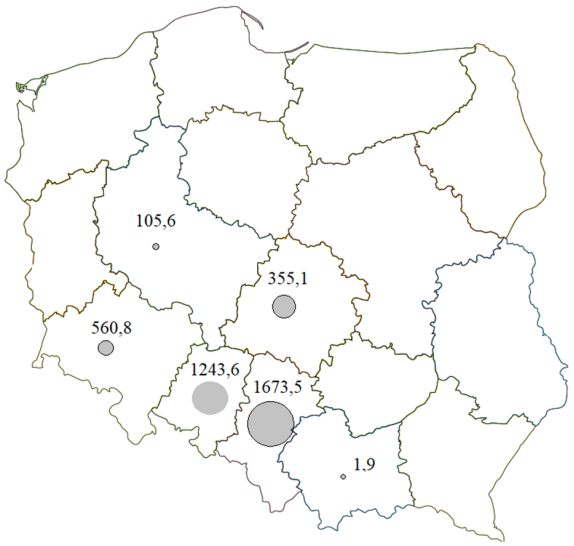

Fig. 5. Wastes (with the elimination of municipal wastes) – stored thus far (gathered) on own dumping grounds (heaps) of foundry plants in 2016 [thousand tons]

The fact that the amount of waste gathered in the dumping grounds of foundry plants has decreased successively throughout the whole country constitutes a positive prognosis. This may be related to the rapidly escalating costs of waste storage. Within the tested years, the amount of gathered waste (on the national scale) decreased from 4796.6 thousand tons (in 2010) to 3940.5 thousand tons in 2016. In this year, there is no information on neutralized waste (Fig. 6).

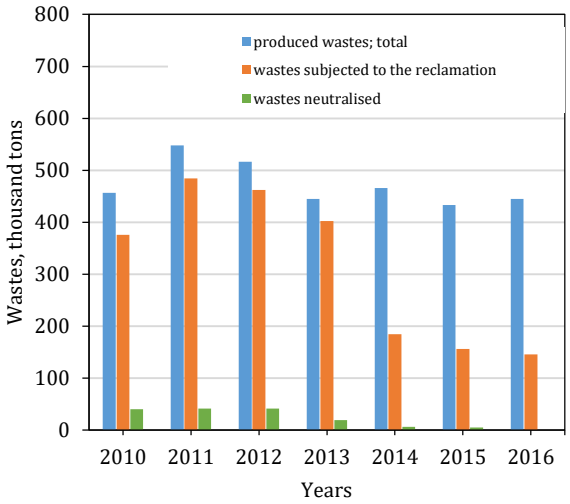

Fig. 6. The compilation of produced wastes, subjected to the reclamation process and neutralised in the period 2010–2016 [21]

Individual groups of wastes produced in the space of the tested years were also analysed. The sequence of their presentation depends on their percentage in the produced wastes.

Apart from the wastes to which spent moulding and core sands belong, there are also wastes originating from the pouring process, marked with code 10 09 08. Data gathered up to the year 2013 indicates that the ratio of the amount of produced wastes to those subjected to the reclamation

process was at a similar level and amounted to 44.7 thousand tons. A regression was observed in 2014 and which remained over subsequent years. The diagrams showing amounts of produced and reclaimed wastes in individual years are presented in Figure 7.

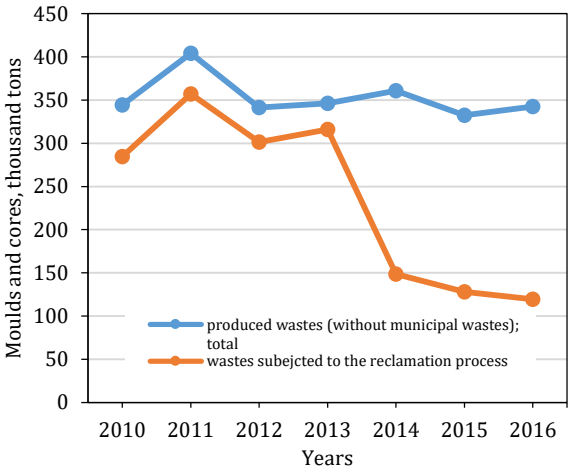

Fig. 7. Listing the amount of waste from the technology of forms and cores in 2010–2016 [21]

In the period studied, it was only in the year 2012 that the production of wastes from the group marked as 10 09 07, was revealed. These are cores and moulds after the pouring process containing dangerous substances. All of these wastes were subjected to reclamation procedures. This means that – according to the available data – foundry plants do not have waste in their dumping grounds from the group no. 10 09 07. Hazardous wastes gathered by foundry plants are dusts from exhaust gases containing dangerous substances.The amount of this waste, marked by code 10 09 09, was at a constant level of 1.2 thousand tons during the study period.

On the next places of waste produced by the foundries there are slags and dusts (Figs. 8 and 9). Also in their case, up to the year 2013 a constant difference between produced and reclaimed wastes could be noticed. After this year, there was a significant decrease in the amount of waste recovered.

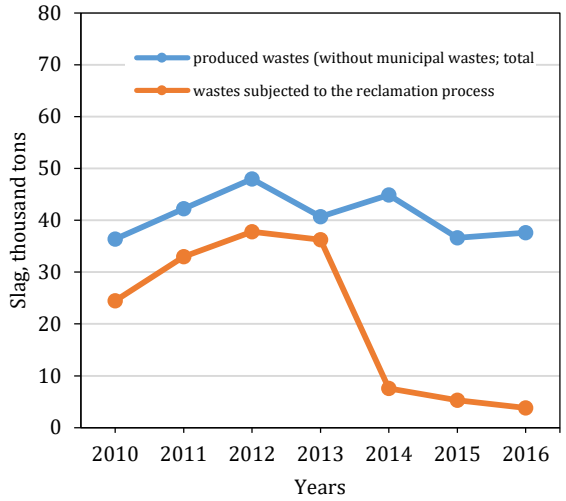

Fig. 8. Slag from the liquid metals melting produced in years 2010–2016 [21]

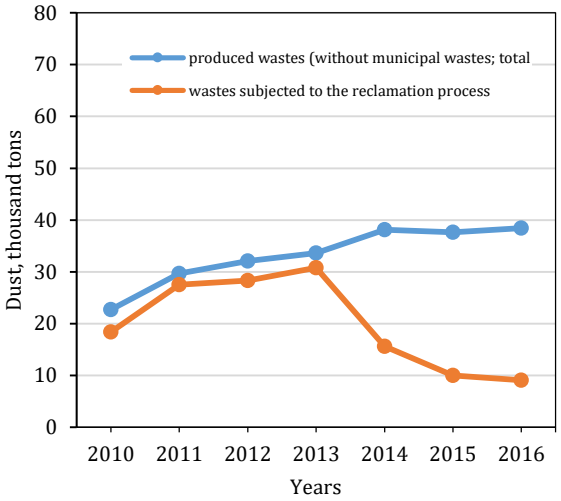

Fig. 9. Dusts from dedusting furnaces for melting liquid metals in years 2010–2016 [21]

3. CONCLUSIONS

The following conclusions can be drawn on the basis of the analysis:

- The ratio of the wastes produced during the pouring processes to the wastes subjected to the reclamation processes was at a similar level in years 2010–2013.
- An alarming decrease of waste subjected to reclamation was observed in 2014. However, it could have been caused by a change in the classification method of the waste produced, with it being delivered to other customers and not subjected to reclamation procedures and neutralised.
- In 2014–2016, a further decline in the amount of waste subject to remediation can be observed.

REFERENCES

[1] Holtzer M., Dańko R., Dańko J., Kubecki M., Bobrowski A. & Śpiewok W. (2013). *Ocena szkodliwości materiałów wiążących stosowanych do mas formierskich i rdzeniowych nowej generacji.* Kraków: Wydawnictwo Naukowe Akapit.

[2] Meléndez A., García E., Carnicer P., Pena E. & Larrión M. (2012). Fine and Ultrafine Emission Dynamics from a Ferrous Foundry Cupola Furnace. *Journal of the Air & Waste Management Association*, 60(5), 556–567. doi:10.3155/1047-3289.60.5.556

[3] Maj M., Werrtz J. & Piekło J. (2017). Environmental Protection Versus Foundry Engineering Practice. *Archives of Foundry Engineering*, 17(2), 202–206.

[4] Dutouquet C., Gallou G., Le Bihan O., Sirven J. B., Dermigny A., Torralba B. & Frejafon E. (2014). Monitoring of heavy metal particle emission in the exhaust duct of a foundry using LIBS. *Talanta,* 127, 75–81. Doi:10.1016/j.talanta.2014.03.063

[5] LaFay V., Neltner S., Carroll D. & Couture D.J. (2010). Know the Environmental Impact of Your Additives. *Modern Casting*, 10, 27–29.

[6] Kubecki M. (2016). *Oznaczenie wybranych niebezpiecznych zanieczyszczeń powietrza, generowanych w procesie termicznego rozkładu mas formierskich z żywicami furanowymi.* Doctoral Dissertation. Polska Akademia Nauk, Oddział Katowice, Komisja Odlewnictwa.

[7] Ribeiro M.G. & Filho W.R.P. (2006). Risk assessment of chemicals in foundries: The International Chemical Toolkit pilot-project. *Journal of Hazardous Materials*, 136(3), 432–437. Doi:10.1016/J.JHAZMAT.2006.01.019

[8] Faber J. & Perszewska K. (2017). Identification Odor Compounds Emitted During the Heating of Molding Sands. *Archives of Foundry Engineering,* 17(2), 178–182. Doi:10.1515/afe-2017-0071
[9] Kubecki M., Holtzer M., Bobrowski A., Dańko R., Grabowska B. & Żymankowska-Kumon S. (2018). Analysis of the Compounds from the BTEX Group, Emitted During Thermal Decomposition of Alkyd Resin. *Archives of Foundry Engineering,* 12(3), 69–74. Doi:10.2478/v10266-012-0084-z
[10] Moryson G. (2009). Evaluation classification in the wastes of aluminum and its alloys. Archives of Mechanical Technology and Automation, 29(3), 59–72.
[11] Holtzer M., Dańko R. & Żymankowska-Kumon S. (2012). Foundry Industry – Current State and Future Development Casting Production. *Metalurgija,* 51(3), 337–340.
[12] Dańko J., Dańko R. & Holtzer M. (2003). Reclamation of used sands in foundry production. *Metalurgija*, 42(3), 173–177.
[13] Pezarski F., Maniowski Z. & Izdebska-Szanda I. (2004). Praktyczne aspekty procesu regeneracji piasków z zużytych mas formierskich i rdzeniowych. *Archiwum Odlewnictwa*, 4(13), 171–176.
[14] Łucarz M. (2015). Thermal reclamation of the used moulding sands. *Metalurgija*, 54(1), 109–112.
[15] Dańko R. (2012). Investigations of the matrix quality in the circulation process of moulding sands with an organic binder. *Archives of Foundry Engineering*, 12(1), 21–26.
[16] Skrzyński M. & Dańko R. (2014). Assessment of the Destruction Degree of the Quartz Matrix in the REGMAS Reclaimer. *Archives of Foundry Engineering*, 14(1), 17–22.
[17] Holtzer M., Dańko R., Żymankowska-Kumon S. & Kamińska J. (2009). Assessment of the possibility of utilisation of used ceramic moulds originated from the investment casting technology. *Archives of Foundry Engineering*, 9(2), 159–164.
[18] Joseph M. K., Banganayi F. & Oyombo D. (2017). Moulding Sand Recycling and Reuse in Small Foundries. *Procedia Manufacturing*, 7, 86–91. Doi:10.1016/J.PROMFG.2016.12.022
[19] Dańko J., Kamińska J. & Skrzyński M. (2013). Reclamation of spent moulding sands with inorganic binders in the vibratory reclaimer REGMAS. *Archives of Metallurgy and Materials*, 58(3), 993–996. Doi:10.2478/amm-2013-0117
[20] Kamińska J. (2013). *Analiza wpływu parametrów pracy granulatora misowego na przebieg procesu granul owania pyłów poregeneracyjnych.* Doctoral Dissertation, Kraków: Wydział Odlewnictwa University of Science and Technology, Faculty of Foundry Engineering, Krakow.
[21] *Waste (excluding municipal waste) by Waste Classification. Statistics Poland*. Retrieved from http://swaid.stat.gov.pl/Stan-OchronaSrodowiska_dashboards/Raporty_predefiniowane/RAP_DBD_SROD_6.aspx
[22] 46th Census of World Casting Production. (2012). *Modern Casting*, 25–29.
[23] 47th Census of World Casting Production. (2013). *Modern Casting*, 18–23.
[24] 45th Census of World Casting Production. (2011). *Modern Casting*, 16–21.
[25] 48th Census of World Casting Production. (2014). *Modern Casting*, 17–21.
[26] 49th Census of World Casting Production. (2015). *Modern Casting*, 26–31.
[27] 50th Census of World Casting Production. (2016). *Modern Casting*, 25–29.
[28] Census of World Casting Production: Global Casting Production Growth Stalls. (2017). *Modern Casting*, 24–29.